Nat. Hazards Earth Syst. Sci. Discuss., https://doi.org/10.5194/nhess-2018-192
Manuscript under review for journal Nat. Hazards Earth Syst. Sci.
Discussion started: 26 July 2018

Natural Hazards and Earth System Sciences
Discussions

Development and validation of the Terrain Stability model for assessing landslide risk during heavy rain infiltration

1. Alfonso Gutiérrez-Martín[1] Miguel Ángel Herrada[2], José Ignacio Yenes Gallego[3], Ricardo Castedo Ruiz[4]

[1] Dr. Arquitecto, Escuela Superior de Arquitectura; Universidad de Málaga, España. E-mail: alfonso@coamalaga.es

[2] Catedrático de Universidad, Escuela Superior de Ingenieros de la Universidad de Sevilla. España. E-mail: herrada@us.es

[3] Dr. Ingeniero José Ignacio Yenes Gallego, Jefe de Unidad, Dirección General de Infraestructuras, MINISDEF, Madrid, España. E-mail: jyengal@et.mde.es

[4] Dr. Ingeniero Ricardo Castedo Ruiz, Departamento de Ingeniería Geológica y Minera, Universidad Politécnica de Madrid, España. E-mail: ricardo.castedo@upm.es

Abstract

Slope stability is a key topic, not only for engineers but also for politicians, due to the considerable monetary and human losses that landslides can cause every year. In fact, it is estimated that landslides have caused thousands of deaths and economic losses amounting to tens of billions of euros per year around the world. The geological stability of slopes is affected by several factors, such as climate, earthquakes, lithology and rock structures, among others. Climate is one of the main factors, especially when large amounts of rainwater are absorbed in short periods of time. Taking into account this issue, we developed an innovative analytical model using the limit equilibrium method supported by a geographic information system (GIS). This model is especially useful for predicting the risk of landslides in scenarios of heavy unpredictable rainfall. A hydrological steady-state assumption was incorporated into this approach. The model, called Terrain Stability (TS), was developed and programmed in MATLAB. This model allows a simulation of the slope stability in a 2D spatial distribution. Many variables measured in the field – topography, precipitation, type of soil – can be added, changed or updated using simple input parameters. To validate the model, we applied it to a real example, that of a landslide which resulted in human and material losses (collapse of a building) at Hundidero, La Viñuela (Málaga) in February 2010.

Keywords: Emergencies, stability, rainfall, landslides, critical.

1. Introduction

Until the 1980s, most stability analyses were performed by graphical methods or by using manual calculators. Nowadays, the quickest and most detailed analyses can be performed using any ordinary computer [Wilkinson et al., 2002]. Currently, the vast majority of stability analyses are performed with commercial software like Slide, SLOPE/W, Phase2, GALENA, GSTABL7 and GEO5 [Gonzalez de Vallejo et al., 2002]. These programmes are used to follow

breakage and circular failures, even reaching as far as the cliff toe, to provide the critical FOS. However, these programmes have some limitations. First, they require a payment license and can be expensive. Second, their calculations are restricted to limited initial parameters which are, in general, not very interactive.

For the stability analysis, different approaches can be used, such as the limit equilibrium methods [Cheng et al., 2007; Liu et al., 2015], the finite elements method [Griffiths et al., 2007; Tschuchnigg et al., 2015; Griffiths, 2015] and the dynamic method [Jia et al., 2008], among others. Limit equilibrium methods are well known, and their use is simple and quick. These methods allow us to analyse almost all types of landslides, such us translational, rotational, topple, creep and fall, among others. Also, limit equilibrium methods can be combined with probabilistic techniques [Stead et al., 2000] or with other models, like stability analysis of coastal erosion [Castedo et al., 2012]. However, they are limited in general to 2D planes and easy geometries. Numerical methods – finite elements methods – give us the most detailed approach to analysing the stability conditions for the majority of evaluation cases, including complex geometries and 3D cases. Nevertheless, they present some problems, such as their complexity, data introduction, mesh size effect and the time and resources they require [Ramos Vásquez, 2017].

Software such as the programmes mentioned above provide useful tools for determining the stability FOS and for giving the most probable breakage (shearing) surfaces. This technique is fast and allows the field or emergency engineer to make timely decisions. Although this methodology is only available in some current software (Slide V 5.0, STB 2010, Geo-Slope), and based on limit equilibrium methods, it is highly recommended because of its reliability for representing real conditions in the field [Chugh, 1981]. While these software programmes can reproduce the actual water table, they cannot reproduce the effect of matrix suction caused by rain infiltration [Herrada et al., 2014]. This rain infiltration produces a substantial reduction of cohesion (a key soil parameter for stability) that cannot be reproduced by actual software and then several real situations cannot be predicted.

Delft University has developed a well-known and free software programme to analyse landslides, the STB 2010 [Verruijt, 2010]. This programme is based on a limit equilibrium technique, using a modified version of Bishop's method to calculate the FOS only for circular failures. It is a user-friendly tool, but it does not allow the calculation of water infiltration on a hillside. This is a critical point, as it is well known that rainfall infiltration is one of the main causes of landslides worldwide [Michel et al., 2015]. Reviewing these issues, a new solution must be developed for cases where landslides are linked to heavy rainfall. In this study, we developed a new model and programmed it using MATLAB. The primary result of this model was a stability index, namely the minimum FOS, *Fs,* based on the limit equilibrium technique, in this case the Bishop's method. The model also provides a possible failure curve, which can be used to coincide with analysis of the actual event as tested with field data. Topographical data can also be introduced into the model from the digital elevation model (DEM) in a GIS.

Nat. Hazards Earth Syst. Sci. Discuss., https://doi.org/10.5194/nhess-2018-192
Manuscript under review for journal Nat. Hazards Earth Syst. Sci.
Discussion started: 26 July 2018

Natural Hazards and Earth System Sciences
Discussions

2. Terrain Stability model development

In the model we developed, we used the limit equilibrium technique for its versatility, calculation speed and accuracy. An analysis can be done studying the whole length of the breakage (shearing) zone or just small slices. Starting with the original method of slides developed by Petterson and Fellenius (1936), some methods are more accurate and complex [Spencer 1967, Morgenstern and Price, 1965] than others [Bishop, 1955 and Janbú, 1954]. Using Spencer's method [Spencer, 1967; Chung 1986] here would mean dividing our slope into small slices that must be computed together. This method is divided into two equations, one related to the balance of forces and the other to momentum. Spencer's method imposes an equilibrium not only for the forces but also for the momentum on the surface of the rupture. If the forces for the entire soil mass are in equilibrium, the sum of the forces between each slice must be also equal to zero. Therefore, the sum of the horizontal forces between slices must be zero as well as the sum of the vertical ones (equations 1 and 2).

$$\sum[Q\cos\theta] = 0 \quad (1)$$

$$\sum[Q\sin\theta] = 0 \quad (2)$$

In this equation, Q is the resultant of the pair of forces between slices, and θ is the angle of the resultant (Figure 1). From this, it can be stated that the sum of the moments of the forces between slices around the critical rotation centre is zero:

$$\sum[QR\cos(\alpha-\theta) = 0] \quad (3)$$

This takes into account that the sliding surface is considered circular, so the radius of the curvature is constant and can be extracted.

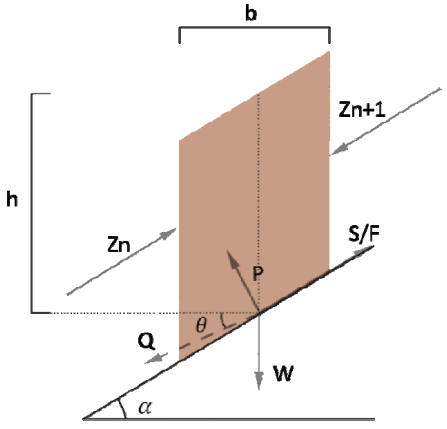

Figure 1. *Representation of the forces acting on a slice, considered in Spencer's method [Spencer, 1967]. W is the external vertical loads; Zn and Zn+1 are the forces acting on the left- and right-hand side of each slice, respectively, with their horizontal and vertical components; P and S are the normal and tangential forces at the base of the slice.*

Nat. Hazards Earth Syst. Sci. Discuss., https://doi.org/10.5194/nhess-2018-192
Manuscript under review for journal Nat. Hazards Earth Syst. Sci.
Discussion started: 26 July 2018

Natural Hazards and Earth System Sciences
Discussions

These equations must be solved to get the FOS, (F_S), and tilt angles of the forces among the slices (θ). To solve these equations, an iterative method is required until a limiting error is reached. Once F_S and θ are calculated, the remaining forces are also obtained for each slice. Spencer's method is considered very accurate and suitable for almost all kinds of slope geometries and may be the most complete equilibrium procedure. It may also be the easiest method for obtaining the FOS [Duncan and Wright, 2005]. Depending on the type of slope analysed, this model is able to establish the failure curve following the typical rotational circle, among other uses [Verruijt, 2010].

The FOS, F_S, classically defined as a ratio of stabilizing and destabilizing forces, determines the stability of a slope as follows:

$$F_S = \frac{\sum(Forces\ standing\ against/oppose\ sliding)}{\sum(Forces\ that\ induce\ sliding)} \quad (4)$$

According to limit equilibrium methods, the two equilibrium conditions (forces and moments) must be satisfied. Spencer's method [Spencer, 1967] is more precise and simple in the TS model. Taking into account these elements, the FOS is then obtained from the following expression:

$$Fs = \frac{1}{\sum W \sin\alpha} \sum[c'b \sec\alpha + \tan\phi' \ (W\cos\alpha - ub\sec\alpha)] \quad (5)$$

According to equations (4) and (5), the slope FOS (F_S) can be considered unstable if its value is lower than 1, or stable if it is higher than 1. It should be noted that, when applying the factor in the engineering and architecture fields, the limiting value tends to be higher than 1, with common values being 1.2 or even up to 1.5 [Burbano et al., 2009]. This is just a confidence measure for your calculations. The FOS can also be defined as the ratio between the shear strength (τ), based on the cohesion and the angle of friction values, and the shear stress, based on the cohesion and the internal friction angle required to maintain the equilibrium (τ_{mb}).

As mentioned, the minimum FOS to consider a talus stable is equal to 1. However, several authors [Yong et al., 1977; van Westen and Terlien, 1996] suggest that the angle of a slope would have to be defined by a value of the FOS superior to unity to take into account the exogenous factors of the slope. Following Jimenez Salas [1981], a value of $F_S \geq 1.3$ can be considered stable by most standards.

To analyse the slope using the Spencer's method, a set of equations must be solved to satisfy the forces and momentum equilibrium and to obtain the F_S. The values of F_S and θ are the unknowns that must be solved. Some authors suggest that the variation of θ can be arbitrary

142 [Morgenstern y Price, 1965], although the effect of these variations in the final value of F_S is
143 minimal. The variation of the angle depends on the soil's ability to withstand only a small
144 intensity of the shear stress.

145 Having said that, if we assume that the forces between slices are parallel (in other words, that
146 θ is constant), equations (1) and (2) become the same, resulting in:

147

148 $$\sum Q = 0 \qquad 6$$

149 The assumption that the forces between slices are parallel gives optimal results for the
150 calculation of the critical safety coefficients in equation 5 [Spencer 1967]. To solve these
151 equations, we used the FSOLVE function of the MATLAB software, giving an initial FOS and
152 angle. The FSOLVE function is a tool inside the optimization toolbox from MATLAB that solves
153 systems of nonlinear equations. When using this tool, an initial value must be provided to start
154 the calculation.

155

156 The application of a homogeneous pore pressure distribution (permanent interstitial pressure)
157 has been included in the model [Bishop and Morgenstern, 1960]. In this case, the permanent
158 interstitial pressure on the base of the slice was determined by the following expression:

159

160 $$u = r_u \gamma h \qquad 7$$

161 In this expression, u is the pore pressure (permanent interstitial pressure) at the base of the
162 slice, and the weight of it affects the W evaluation. The factor r_u is a coefficient of pore
163 pressure (interstitial pressure coefficient), which determines the rain infiltration factor on the
164 slopes. As it is well known, the water that infiltrates the soil may produce a modification of the
165 pore pressure, affecting its resistant capacity. This factor may vary from 0 (dry conditions) to
166 0.5 (saturated conditions). Finally, to obtain the pore pressure, u, the Coulomb equation is
167 needed:

168

169 $$S = c + (\sigma - u)\tan\emptyset \qquad 8$$

170 In this equation, S is the tangential shear resistance, c is the cohesion, σ is the normal stress
171 and ϕ is the internal friction angle. To introduce soil shearing parameters like cohesion or the
172 friction angle, a drained status must be considered [Duncan, 1996].

173

174

175

Nat. Hazards Earth Syst. Sci. Discuss., https://doi.org/10.5194/nhess-2018-192
Manuscript under review for journal Nat. Hazards Earth Syst. Sci.
Discussion started: 26 July 2018

Natural Hazards and Earth System Sciences
Discussions

3. Terrain stability (TS) model behaviour tests

Figure 2 shows the results of applying the Terrain Stability model to an irregular slope, including the initial and final points of the first failure circle (shown in yellow). This circle corresponds with the initial value introduced by the user into the FSOLVE function. The points of the talus are extracted from a DEM model in ArcGIS 10 [Glennon et al., 2008]. The talus height is equal to 15 m, and the soil is uniform with the following nominal properties: γ = 19500 N/m^3, ϕ = 22º, c = 15000 N/m^2, u = 0 N/m^2. According to the in situ test carried out by the Geoner SL laboratory, the soil is a silty clay from Gibraltar Flish.

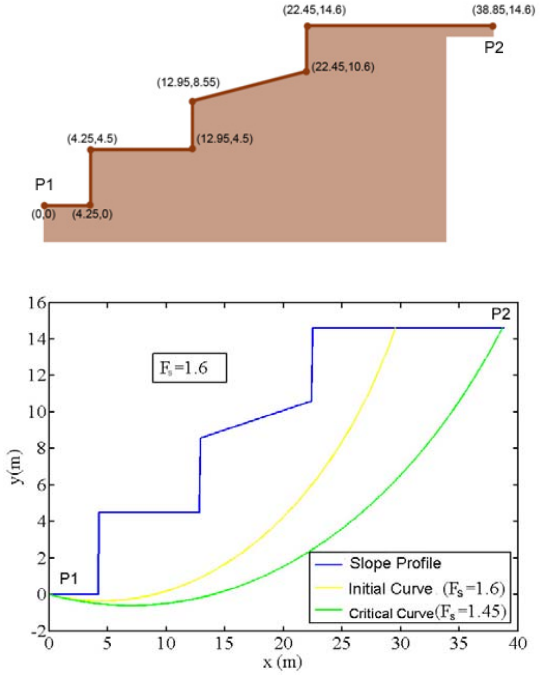

Figure 2. *Results following the application of the software showing the talus profile and surface damage. The F_S and the clearest proof of circular failure are also provided (see the yellow line). P1 coordinates are (0, 0) and P2 (38.85, 14.6) in metres.*

The code works as follows: the initial circular failure curve is plotted using the FPLOT tool, as shown in Figure 2 (yellow line). In this example, the centre coordinates are equal to x_c = 7 m; y_c = 14 m and the lower cut with the talus coordinates (P1 point) equal to x_t = 0 m, y_t = 0 m. The FOS obtained was 1.6, which is, in principle, a stable talus. It must be taken into account that the mass susceptible to slipping must be divided into N pieces equal to the number of slices; in this example, the mass was divided into N = 500 slices.

The next step is to apply Spencer's method to the different breakage surfaces until the curve with the lowest FOS, F_S, is found, and that will be the critical surface susceptible to a circular slip. To determine the minimal FOS using this model, calculate the displacement of the lower cut point of the critical slip from slope, as well as the rotation centre position of the critical failure curve. In addition, a number of potential circular failures must be introduced by the

user. Then, the user introduces the following constraints into the programme: the initial or lower point of the failure curve (P_1) in its intersection point with the slope, which may or may not match the origin of the slope analysed. Another restriction is the centre of the failure circle, (X_0, Y_0), that should initially cut the slope, i.e. the breaking curve must be within the feasible sliding region. With this data, the programme automatically draws a first curve, in this case the yellow line in Figure 2, and calculates the safety coefficient F_s for that initial curve.

On the basis of this first curve (yellow line in Figure 2), the programme enforces new restrictions:

- The curve passes through the origin of slope P1 = (0, 0).
- The centre of the possible circles of critical breakage is inside the rectangular box defined as: ($x_{box\ min.} < x_c < x_{box\ max.}$; $y_{c\ box\ min.} < y_c < y_{box\ max}$). Note that the coordinates are entered with the 2D expression (X, Y).

Both coordinates of the rotation centre position are free and can change for every circle. From the initial failure curve, characterised by the point x = (x_c, y_c), the MATLAB "fmincon" function is used to obtain a new critical point (x_c*, y_c*) where the FOS from the breakage curve is the minimum provided by fmincon. In this example, starting from the initial curve (yellow curve) with point x = (7, 14), the TS model provides a new point x* = (4.4910, 28.1091, 0) with a new FOS, F_S = 1.45. In this case, the new search has been carried out with the following restrictions in the rectangular box, such as 2 m < x_c < 8 m and 16 m < y_c < 40 m. These restrictions are imposed in order to determine the critical circle. With all these restrictions, and because of the first calculated curve (the yellow curve), the developed model calculates the critical curve among the number of curves selected by the user (500 in this case), as well as the failure circle centre, by applying the fmincon (MATLAB function). This defines the curve with a minimum FOS (F_{min}) as the value of F_s (see green curve in Figure 2). When solving this problem, a critical selection is the lower cut-off point of the slope. According to different authors, such as Verruijt (2010) and Castedo et al. (2012), the selected point is the same as the P1 point.

To complete the second phase in the TS model operation, the effect of rain infiltration must be introduced by the coefficient of the pore pressure factor r_u. In this example, the infiltration factor was introduced at the base of each slice to account for the infiltration and pore pressure at the base of the break surface of the slope. If r_u increases, the cohesion of the soil mass of the slope decreases, directly affecting the reduction of the slope's FOS. The result is that a dry talus has a F_S = 1.45, but if including the r_u parameter equal to 0.3, the FOS decreases to a value of F_S = 0.95, that means an FOS below the unity, so an unstable circular failure appears (see Figure 3). Entering the infiltration factor, r_u, in Spencer's method to introduce the infiltration effects in slopes, the geotechnical cutting elements of the analysed soil are reduced, also reducing the values of the F_s, both for the initial yellow curve and the optimum green curve (Figure 2). Note that the initial curve in the run shown in Figure 3 is different from the one in Figure 2, as it depends on the data introduced.

Nat. Hazards Earth Syst. Sci. Discuss., https://doi.org/10.5194/nhess-2018-192
Manuscript under review for journal Nat. Hazards Earth Syst. Sci.
Discussion started: 26 July 2018

Natural Hazards and Earth System Sciences
Discussions

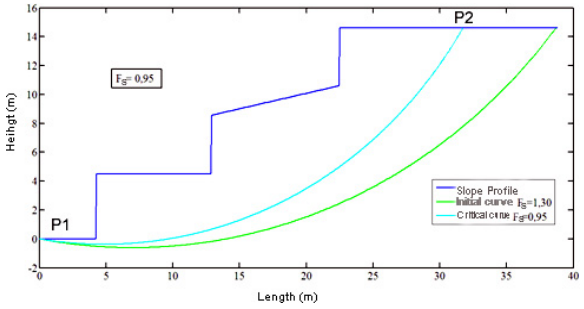

Figure 3. *Outcome of the TS model after the introduction of the infiltration factor, producing an unstable circular failure (Fs = 0.95).*

After the outcome produced here, it can be stated that the rainwater infiltration factor is necessary to predict instabilities in slopes. If this infiltration factor is small enough, taking into account the safety coefficients, the design may still be adequate, but there was a lack of critical information for calculating this parameter.

4. Example of this application in the municipality of La Viñuela, Málaga, Spain

In 2010, La Viñuela, Málaga, Spain experienced experienced torrential rainfall. The main consequence was a devastating landslide with serious personal and material losses, as shown in Figure 4. The coordinates where this event occurred were in degrees (36.88371409801, -4.204982221126).

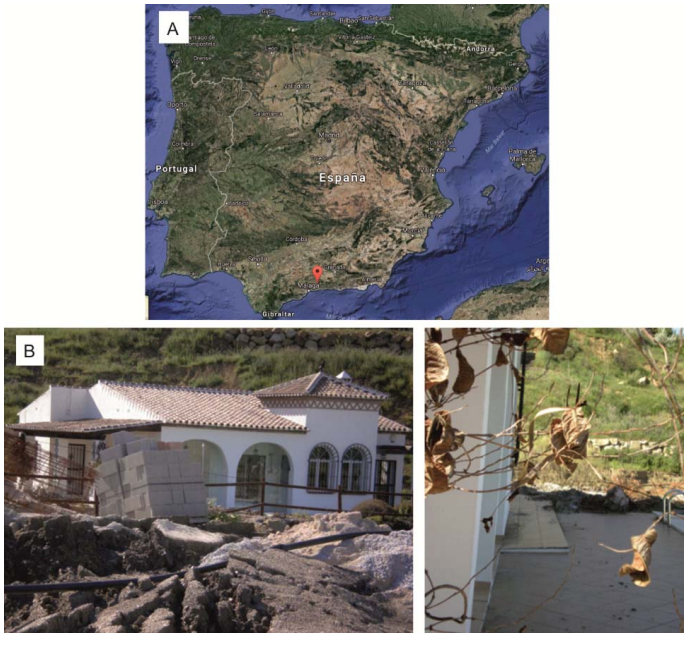

Figure 4. *A) Spanish map with the location of La Viñuela (Google Maps). B) Real images taken by the authors at La Viñuela in 2010.*

Nat. Hazards Earth Syst. Sci. Discuss., https://doi.org/10.5194/nhess-2018-192
Manuscript under review for journal Nat. Hazards Earth Syst. Sci.
Discussion started: 26 July 2018

4.1 Geological and hydrological environment

The study area is located in the county of La Viñuela, specifically in the Hundidero village, which is located immediately north of the Pantano de La Viñuela and south of the Betic mountain range (South Iberian Peninsula).

According to the Cruden and Varnes' classification [1996], the slide suffered in the *Paraje del Hundidero de la Viñuela* corresponds to a rotational slide-like complex movement because it was generated in two sequences at different speeds. This type of mechanism is characteristic of homogeneous cohesive soils, as was the one analysed here.

This event caused serious damage to different buildings. Regarding the damage caused, in the initial stretch of the slope (its head), a house was dragged and destroyed and another was seriously damaged. On the right bank of the mentioned house, another building was affected. In total, this event left a balance of two buildings destroyed and one seriously compromised. Although 15 people lived in these houses, there were no fatalities. About 20 houses were to be constructed at the head of the slope; fortunately, the event happened before this construction. Figure 5 shows an aerial picture from 2006 before the disaster as well as the affected area and landslide in 2010.

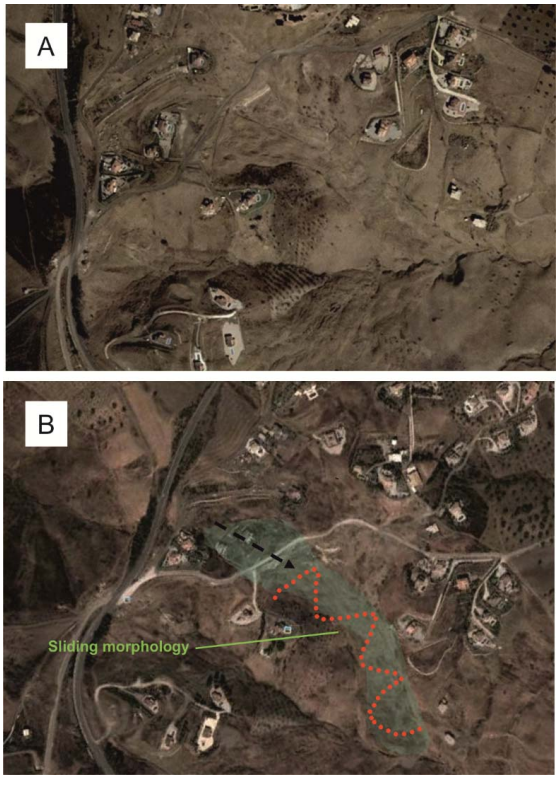

Figure 5. *A) An aerial photograph from before the event (2006). B) An aerial photograph taken after the landslide (2010).*

Nat. Hazards Earth Syst. Sci. Discuss., https://doi.org/10.5194/nhess-2018-192
Manuscript under review for journal Nat. Hazards Earth Syst. Sci.
Discussion started: 26 July 2018

Natural Hazards and Earth System Sciences
Discussions

4.2 Event features and geometry

It is well known that mass movements, such as landslides, are highly complex morphodynamic processes. We selected the Hundidero as our study area because it is prone to landslides. In order to analyse this case study using our model, we first calculated the initial displaced volume of the study area. According to the dimensions of the problem, the initial displaced volume was calculated, equivalent to the volume of half an ellipsoid [Varnes, 1978; Beyer, 1987; Cruden and Varnes, 1996] equal to Vol = 1/6 π (width x length x depth). In our particular case, the width was equal to 70 m, the length equal to 235 m and the depth equal to 5 m, making up a total volume of 4.364 m^3 (Figure 6). Taking an average of 33% elongation, as proposed by Nicoletti and Sorriso-Valvo [1991] and Cruden and Varnes [1996], we determined that the total material displaced in this landslide had an approximate volume of 5.804 m^3. In this mass displacement, it is also necessary to consider material added by erosion and dragged from the initial mass displaced. In Figure 5, the straight line indicates the first rotational movement, and the zigzag line shows the planar drag and glide after the first rotational movement. The green region is the total area displaced or affected by mass movement. After the first circular movement, the mass moved rapidly, associated with a continuous rise in incremental pore pressure and the rapid reduction of shear strength, without allowing pressure dissipation.

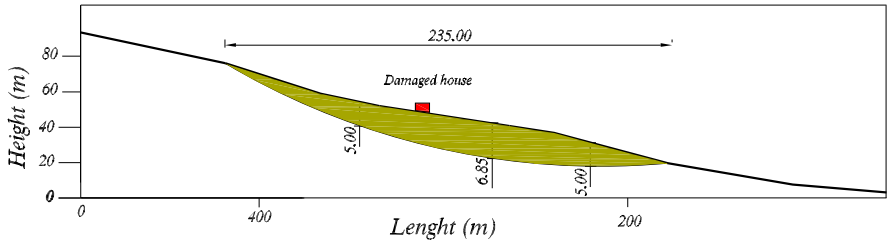

Figure 6*. Characterisation and longitudinal section of the rotational sliding (Geolen S.A., 2010). The location of the dragged house is noted in red. Analysed by the TS model.*

The initial spit of land had an approximate size of 235 m in length by 70 m in width. Due to this initial displacement, there was a drag and a huge posterior planar displacement of about 550 m length, affecting a zone with several parcels of land and buildings. These dimensions were confirmed using aerial photography and field data. The soil is basically composed of clays of variable thicknesses, of fine grain, with fluvial sediments and silty clay. The authors obtained this data by conducting a field survey, as well as through the laboratory tests carried out by the laboratory Geolen S.A. [Geolen, 1998]. From a geological and geotechnical point of view, according to a survey of those present as the laboratory extracted the materials, different lithological levels can be distinguished, as shown in Table 1.

Table 1. *Lithology of the area affected by the failure, according to the laboratory tests of Geolen S.A. No groundwater level was detected.*

Level/layers	Lithology	Depth (m)
LEVEL 1	Silty sand with natural schistose pebbles	0.90
	Silty clay with marl intercalations	4.20
LEVEL 2	Colmenar unit, upper oligocene–lower miocene	
	Sandy clay	9.00
LEVEL 3	Colmenar unit, upper oligocene–lower miocene	(*end of the probe*)

The laboratory tests included a sieve analysis (following UNE 103 101) in three of the samples extracted from the field, at depths of 1.80–2.00 m, of which 70.3% was composed of clay and silt; according to this, the sample is classified as cohesive. The liquid limit and the plastic limit were determined on two of the samples (following UNE 103 103 and UNE 103 104, respectively), yielding liquid limit values of 57.5% and 64.2% and a plasticity index of 37%, respectively. According to the lab results, the material can be classified as high plasticity material with the potential of having a high water content. However, based on the field inspection and the analysis of the rainfall series in the La Viñuela region in 2010 (see Figure 7), it can be inferred that the main causes of the event were:

- the poor geomechanical parameters of the material that formed the affected hillside, and
- the hydrometeorological conditions in the days preceding and days after the event, according to the histogram.

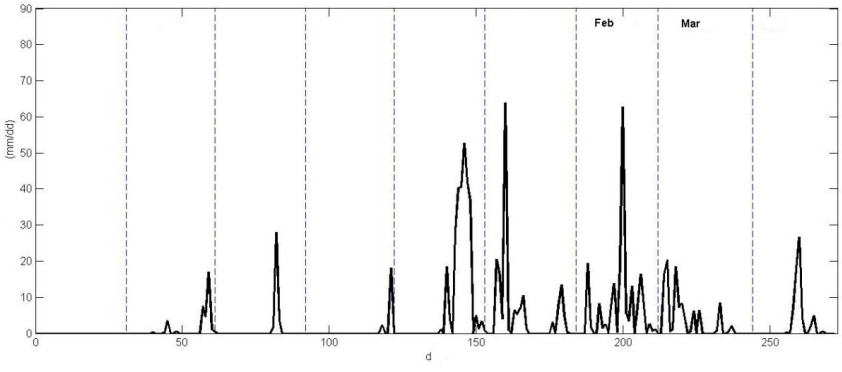

Figure 7. *Rainfall histogram at La Viñuela from August 2009 to April 2010.*

Most of the landslides observed during these days occurred as a consequence of exceptionally intense rainfalls. The precipitation data was provided by the meteorological station of La Viñuela (Figure 7). It can be observed that large amounts of precipitation fell during the months of December, January, February and March of 2009 and 2010, with peaks of almost 60 l/m^2 in a single day (January). In total, 890 l/m^2 fell to the end of April. This is a key point in

slope stability to consider when dealing with areas capable of having high infiltration rates. The rotational slide analysed had occurred between level 2 and level 3, when the water content reached that depth, as confirmed by the infiltration calculations in the terrain (see graphs in Figure 9, reaching depths of up to 5 m). Two direct shear tests (consolidated and drained) were conducted in unaltered samples extracted from the boreholes at 3.00–3.60 m and 4.00–4.60 deep. The cut-off values of the soil are specified in Table 2. Those values were used in the developed software to obtain the safety coefficient and the theoretical failure curve.

Table 2. *Summary chart of the characteristics of the soil analysed at the GEOLEN S.A. laboratory: ϕ the angle of internal friction, c the cohesion, γ_{Sat} the saturated specific gravity and γ_a the apparent specific gravity.*

Soil parameter	Result	Units
ϕ	17	º
c	0.27	N/mm^2
γ_{Sat}	2000	N/mm^3
γ_a	1650	N/mm^3

The dynamic and continuous tests were carried out by the Geolen S.A. laboratory with an automatic penetrometer ROLATEC ML-60 A type. The data obtained was transcribed by the number of strokes to advance the 20 cms tip, which is called the "penetration number" (N_{20}).

This test is included in the ISO 22476-2:2005 standard as a dynamic probing super heavy, and consists of penetrating the ground with a conical tip of standard dimensions. The depth of the failed mass can be estimated, as well as the theoretical failure curve for an increase in the soil consistency (see data in Table 3).

The change in the geomechanical response of the soil takes place at a depth of 4–5 m, according to the results of N_{20} and US (samples without changes) taken along the analysed column. In this case, the sloped ground mass showed a characteristic striking relationship of a displaced terrain [Gonzalez de Vallejo et al. 2002]. This differs from the underlying or unmoved terrain, which indicated a more consistent striking relationship, that was taken within the area of the landslide behind the house drawn in accordance with the analysis of the hits N_{20} from Table 3.

Table 3. *Summary chart of the soil analysed at the GEOLEN S.A. laboratory. Bold values show, according to the data of the field penetrometers, the depth mobilized by the rotational sliding.*

Depth (m)	Hits N_{20}	Consistency	Admissible stress (N/mm^2)
0.00 – 1.00	**4**	**Soft**	**0.03**
1.00 – 2.00	**3**	**Soft**	**0.02**
2.00 – 3.00	**6**	**Slightly hard**	**0.04**
3.00 – 4.00	**7**	**Slightly hard**	**0.05**
4.00 – 5.00	**10**	**Slightly hard**	**0.07**
5.00 – 6.00	19	Moderately hard	0.12
6.00 – 7.00	52	Hard	0.31
7.00 – 8.00	63	Hard	0.35
8.00 – 8.60	84	Hard	0.44

Nat. Hazards Earth Syst. Sci. Discuss., https://doi.org/10.5194/nhess-2018-192
Manuscript under review for journal Nat. Hazards Earth Syst. Sci.
Discussion started: 26 July 2018

Natural Hazards and Earth System Sciences
Discussions

4.3 Input data

To analyse the topography of the critical section, we obtained the DEM data from ArcGIS 10 software programme [Esri, 2010], with a scale of 1:1000, through Spanish National Geography (IGN) raster maps, with adequate accuracy. These data were interpolated to a 2 m grid using a triangulated network interpolation methodology. Orthophotos proved very useful to locate the landslide with accuracy and to validate the field survey. The model developed here applies to failure in an initiation zone, in addition to predicting landslides, including those induced by the infiltration of critical rains.

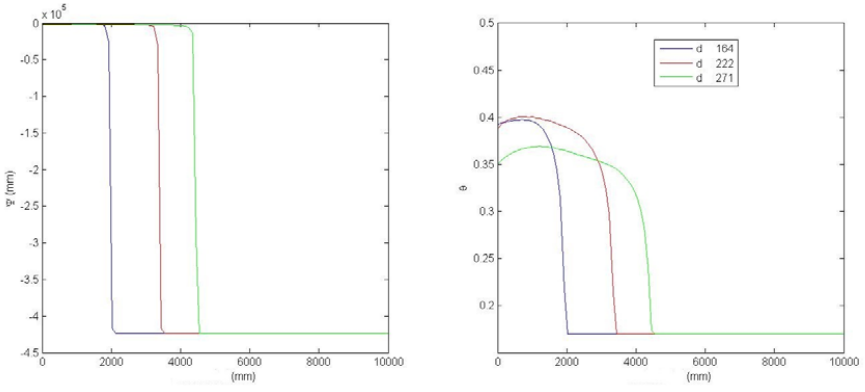

Figure 8. *Left: hydraulic potential. Right: volumetric water content. Both have been plotted as a function of the depth (mm) at different times (d).*

To complete the input data, we plotted the hydraulic potential and the volumetric water content, as a function of depth in the ground for different time steps, using a previously developed infiltration model, as shown in Figure 8 [Herrada et al., 2014]. The figure shows the evolution of how the wetting front advances can be observed. These reached almost 5 m deep at the end of April 2010.

4.3 Analytical results

We applied the TS model using data from the ArcGIS 10 software programme and inventory from the landslide. We did so to obtain the degree of stability of the sliding land based on the angle of internal friction, the cohesion, the density and the angle of the slope we analysed. Figure 9 shows the analytical results from the real talus. In addition we compared the results given by the developed TS model and the results given by STB 2010 model, using free surfaces in both cases. Due to the versatility of our programme, we were able to transfer the initial curve from our previous calculations (shown in yellow) onto this one (shown in red). The worst curve (shown in green) was calculated automatically from the initial curve, resulting in F_S = 2.300, in the dry state.

Nat. Hazards Earth Syst. Sci. Discuss., https://doi.org/10.5194/nhess-2018-192
Manuscript under review for journal Nat. Hazards Earth Syst. Sci.
Discussion started: 26 July 2018

Natural Hazards and Earth System Sciences
Discussions

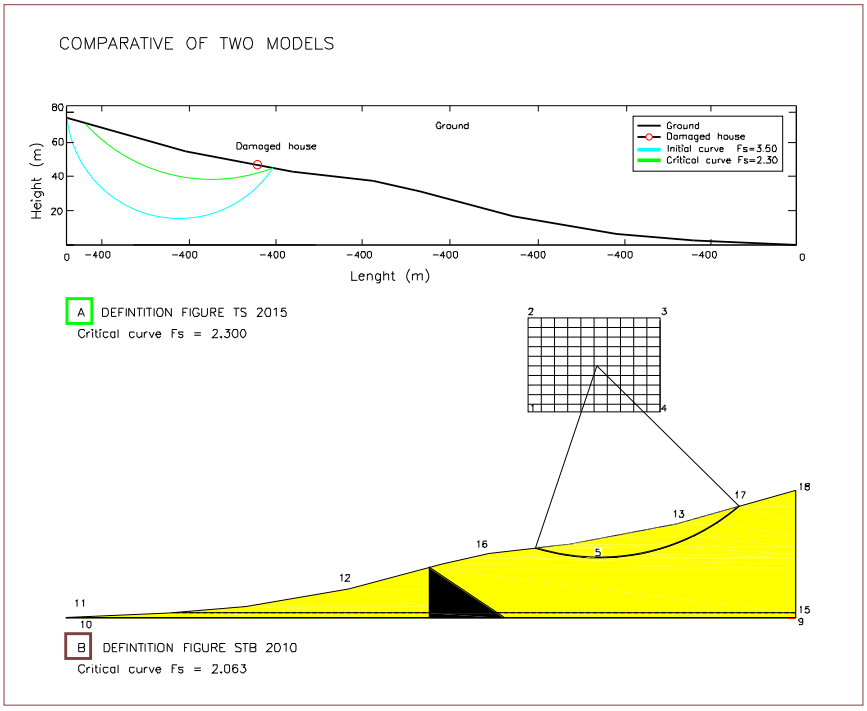

390

391 ***Figure 9.*** *Top: TS model with a critical failure of F_S = 2.300. Bottom: results from the STB 2010 model with*
392 *an FOS of 2.063.*

393 As can be noted, the failure curves are similar, and the safety coefficients F_S only differ by
394 0.237. In both cases, the results indicated are conservative estimates, resulting in a stable talus
395 that was not realistic, as was the case in La Viñuela. In order to get the most unfavourable
396 curve, which would match the analysis of the actual event, the pore coefficient must be
397 introduced. At the first runs of the model, the r_u was equal to zero (dry soil – Figure 9), but if
398 this value is changed to r_u = 0.35, the results are quite different (Figure 10). The resulting
399 failure was near the surface and the top cut with the talus found relatively near the houses.
400 Taking into account the infiltration of rainwater, the slope analysed in the TS model showed a
401 value of F_S = 0.98, in other words, that it was unstable.

402

403 This calculation and the theoretical failure curve provided by our model was able to reproduce,
404 in a realistic way, the landslide which occurred in La Viñuela. Our model found that the critical
405 surface area that corresponded with the profile of the terrain was 12.927.45 m^2, which closely
406 matches the real situation. In the STB 2010 programme, it was 7.825.35 m^2; therefore, our
407 prediction was more precise.

Nat. Hazards Earth Syst. Sci. Discuss., https://doi.org/10.5194/nhess-2018-192
Manuscript under review for journal Nat. Hazards Earth Syst. Sci.
Discussion started: 26 July 2018

Natural Hazards and Earth System Sciences
Discussions

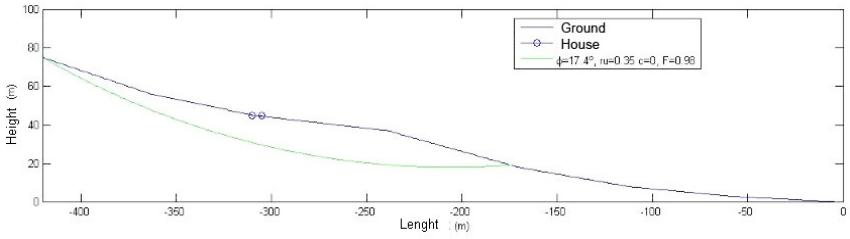

Figure 10. *A new calculation including the pore coefficient r_u showing the worst curve in green. The circles show the house dragged by the landslide.*

As mentioned earlier, the STB 2010 model does not allow stability calculations to apply to rainfall infiltration on a hillside. Hence, it is not capable of predicting a hillside's instability in a critical rainfall scenario, which was critical in the slope analysed. The STB 2010 model found that the hillside studied had an FOS of F_S = 2.063; that means it was a very stable slope. Consequently, our innovative TS model appears to be more efficient and accurate.

The Terrain Stability analysis performed using the developed model defines fairly well the slip-breaking curve that intuitively appears to be susceptible to failure, especially when heavy rains occur. As an example, the landslides which occurred in the La Viñuela area could only have been predicted if the infiltration had been taken into account. Even then, it could not have been done with other available software programmes, which were not able to consider it.

1. In comparison with other software programmes, like the STB 2010, the model developed here can analyse cliffs from right to left and vice versa.

2. Other software programmes, like the STB 2010, use a modified version of Bishop's method, a less precise methodology than Spencer's method. A modified version of Bishop's method solves only the equilibrium in momentum while the Spencer method also considers the equilibrium in forces.

3. Another improvement made by the TS code, in comparison with others, is that the use of the Spencer's method allows us to analyse any type of slope and soil profile. In this procedure, we calculated the worst breaking curve by modifying the calculation points.

4. In the TS model, from the first slip rotational circle obtained in MATLAB, many circles were then calculated using the fmincon function, with some user restrictions. However, other model, like the STB 2010, require the definition of a quadrangular region (to look for the centres of rotational failures) and a point (namely 5, see Figure 9) to define the curve as where the failure must pass. Also, the number of circles that the STB 2010 model can analyse for their minimum value is limited to 100.

5. This model can detect relevant earth movements derived from rainfall infiltration, both translational and rotational types [Stead et al., 2006], such as those that usually occur in regions like India, the United States, South America and the United Kingdom, among other places. The programmes that do not contemplate this option will overestimate the FOS, potentially with great errors.

6. Our model programme has another advantage: it also offers the opportunity to incorporate, in the same code, the stability analysis and the effect of the infiltration factor in the rainfall regime. This is a step forward from open access programs, such as STB 2010, and also alternative payment software, such as Slide.

5. Conclusion

The terrain stability (TS) analysis defines fairly well areas that intuitively appear to be susceptible to landslides and defines rigorously the failure curve and the slip factor of safety (FOS). We developed this model due to the necessity of a useful tool to predict landslides, especially when heavy rains occur.

The TS model we developed uses the Spencer's method, which is more precise than the modified Bishop method, so it differs in the results it provides for the FOS F_S. It also takes into account the factor of water infiltration due to critical rains, which other software programmes do not consider. A failure surface can be determined by constraints using the MATLAB function fmincon. The data needed to run the model include soil and climate properties that may vary in space and time. The exit indices of the analysis (F_S) should be interpreted in terms of relative risk. The methods implemented in the TS model are based on data structures, which are based on the data entry of the elevation model (DEM), key to obtaining the profile to be studied.

In the case study analysed, the hillside was initially stable and was so determined by the analysis performed with the STB 2010 model. However, the hillside became unstable due to the heavy rains of that hydrological period, which called for the application of the pore pressure coefficient r_u. For analysing cases of heavy rain, this model is probably the most powerful tool for determining slope stability. In addition, thanks to the great versatility of this model, it is applicable to any analysis in other parts of the world, based on the methods of limit equilibrium (Spencer 1967). The TS model can also be used in combination with GIS software, SINMAP and aerial photographic analysis, as well as mapping techniques or even as part of other models like the coastal recession models [Castedo et al., 2012].

6. References

Aenor Institut (2008). Geotechnical investigation and testing - Field testing - Part 2: Dynamic probing (ISO 22476-2:2005). Madrid. Spain.

Bishop, A. W., Morgenstern, N. R. (1960). Stability coefficients for earth slope. Geotechnique 10, 129-150.

Bishop, A. W. (1955). The Use of the slip circle in the Stability Analysis of Slope. Geotechnique 5: 1:7-16.

Beyer, W.H. (1987). Handbook of Mathematical Sciences. 6th ed., Boca Raton/Florida

Burbano G., del Cañizo L., Gutiérrez J. M., Fort L., Llorens M., Martínez M., Paramio J. R., Simic D. (2009). Guía de cimentaciones en obras de carretera. Ministerio Fomento: Madrid.

Castedo, R., Murphy, W., Lawrence, J., & Paredes, C. (2012). A new process–response coastal recession model of soft rock cliffs. Geomorphology, 177, 128-143.

Cheng, Y. M., Lansivaara, T., Wei, W. B. (2007). Two-dimensional slope stability analysis by limit equilibrium and strength reduction methods. Computers and Geotechnics 34, Nº 3, 137-150.

Chugh, A. K., Smart, J. D. (1981). Suggestions for slope stability calculations. Computers & Structures 14, 1–2, 43-50.

Cruden, D. M. and Varnes, D. J. (1996). Landslides types and processes. In: Landslides investigation and mitigations. Transportation Research Board Special report 24. Turner y Shuster (eds.), 36-75.

Duncan, J. M., Wright S. G. (2005). Soil Strength and Slope Stability. John Wiley, Hoboken, N. J.

Duncan, J. M. 1996. Landslide Types and Processes. Landslides investigations and mitigation. Ed. Turner A. Special Report, TRB.

Environmental Systems Research. (1969-2017). Institute Geographic information system (platform and resources ArcGIS). California, EEUU. Recovered in http://www.esri.es/arcgis/productos/.

Fellenius W. (1936). Calculation of the stability o Heat dams. Washington, D.C.: In Proceeding of the 2nd Internacional Congress on Large Dams, - Vols. 4, 445. -4:445.

Geolen Engineering. (2010). Geotechnical study in the Viñuela. Sevilla, Spain. Recovered in http://www.geolen.es

Glennon, R., Harlow, M., Minami, M., Booth, B. (2008). ArcGis 9. ArcMap Tutorial. Esri North Carolina. U.S.A.

González de Vallejo, L., Ferrer, M., Ortuno, L., y Oteo, C. (2002). Ingeniería Geológica. Madrid: Prentice Hall.

Griffiths, D. V., Marquez, R. M. (2007). Three-dimensional slope stability analysis by elasto-plastic finite elements. Géotechnique 57, Nº. 6, 537–546.

Griffiths, D. V. (2015). Slope stability analysis by finite elements. A guide to the use of Program slope64. Geomechanics Research Center Colorado School of Mines. (http://inside.mines.edu/~vgriffit/slope64/slope64_user_manual.pdf).

Herrada, M. A., Gutiérrez-Martin, A., Montanero, J. M. (2014). Modeling infiltration rates in a saturated/unsaturated soil under the free draining condition. Journal of Hydrology, 515, 10–15.

Jiménez Salas J.A., Justo Alpañes, J.L. (1981). Geotecnía y Cimientos II. Ed. Rueda. Madrid.

Janbu, N. (1954). Stability analysis of slopes with dimensionless parameters. In: Harvard University soil mechanics series, vol 46.

514 Jia, G. J., Tian, Y., Liu, Y., Zhang, Y. (2008). A static and dynamic factors-coupled
515 forecasting model of regional rainfall-induced landslides: A case study of Shenzhen. Science
516 China: Technological Sciences 51. Suppl. 2, 164-175.

517 Liu, S. Y., Shao, L. T., Li, H. J. (2015). Slope stability analysis using the limit equilibrium
518 method and two finite element methods. Computers and Geotechnics 63, 291-298.

519 Michel. G. P., Kobiyama, M., Fabris, R. (2014). Comparative analysis of SHALSTAB and
520 SINMAP for landslide susceptibility mapping in the Cunha River basin, southern Brazil. Journal
521 of Soils and Sediments 7. 1266–1277.

522 Michel. G. P., Kobiyama, M., Fabris, R. (2015). Critical rainfall to trigger landslides in
523 Cunha River basin, southern Brazil. Natural Hazards 75, 2369-2384.

524 Morgenstern, N. R., Price, V. E. (1965). The analysis of the stability of general slip
525 surfaces. Geotechnique 15, 79-93.

526 National Geographic Institute. (1870-2017). Geological and raster maps. Madrid, Spain.
527 Recovered in http://www.ign.es/web/ign/.

528 Nicoletti, P. G., Sorriso-Valvo, M. (1991). Geomorphic controls of the shape and
529 mobility of rock avalanches. GSA Bulletin 103 (10): 1365-1373.

530 Ramos Vásquez, A. A. (2017). Análisis de estabilidad de taludes en rocas. Simulación
531 con LS-DYNA y comparación con Slide. *Trabajo Fin de Máster*, Máster Universitario en
532 Ingeniería Geológica, ETSI Minas y Energía, Universidad Politécnica de Madrid.

533 Spencer, E. (1967). A method of analysis of analysis of the stability of embankments
534 assuming parallel interslice forces. Géotechnique 17, 11-26.

535 Stead, D., Eberhardt, E., Coggan, J. S. (2006). Developments in the characterization of
536 complex rock slope deformation and failure using numerical modelling techniques. Engineering
537 Geology 83. 1-3:217-235.

538 Tschuchnigg, F., Schweiger, H. F., Sloan, S.W. (2015) Slope stability analysis by means
539 of finite element limit analysis and finite element strength reduction techniques. Part II: Back
540 analyses of a case history. Computers and Geotechnics 70, 178-189.

541 Van Westen, C. J., Terlien, M. J. T. (1996) An approach towards deterministic landslide
542 hazard analysis in gis. A case study from manizales (Colombia). Earth Surface Processes and
543 Landforms 21. 9:853-868.

544 Varnes, D.J. (1978). Slope movement types and processes. In R.L. Schuster y R. J. Krizek
545 (Eds.) Landslides: analysis and control. Transportation Research Board. Special report 176: 11-
546 33.

547 Verruijt, A. (2010). STB—slope stability analysis program. Delft University.
548 (http://geo.verruijt.net).

549 Wilkinson P.L., Anderson M.G., Lloyd D.M., Renaud P-N. (2002). Landslide hazard and
550 bioengineering: towards providing improved decision support through integrated numerical
551 model development. Environment Modelling and software 17:4, 333-344.
552
553 Yong, R. N., Alonso, E., Tabba, M. M., Fransham, P. B. (1977). Application of Risk
554 Analysis to the Prediction of Slope Stability. Canadian Geotechnical Journal 14, 540-553.